Received: 13 April 2020 | Revised: 11 July 2020 | Accepted: 22 July 2020

DOI: 10.1002/qua.26432

FULL PAPER

International Journal of QUANTUM CHEMISTRY WILEY

Influence of H_2O and NH_3 on the reaction of HO_2 with NO in troposphere: Theoretical investigation of HNO_3 formation pathways

Rui Wang[1,2] | Yongqi Zhang[1,2] | Aizhen Li[1] | Mingjie Wen[1,2] | Zerong Geng[1] | Ximei Geng[1] | Zhuqing Wang[3] | Zhiyin Wang[1] | Makroni Lily[4]

[1]Shaanxi Key Laboratory of Catalysis, School of Chemical and Environment Science, Shaanxi University of Technology, Hanzhong, China

[2]Shanghai Key Laboratory of Molecular Catalysis and Innovative Materials, Fudan University, Shanghai, China

[3]Analytical and Testing Center, Sichuan University of Science and Engineering, Zigong, China

[4]Key Laboratory for Macromolecular Science of Shaanxi Province, School of Chemistry and Chemical Engineering, Shaanxi Normal University, Xi'an, China

Correspondence
Rui Wang, Shaanxi Key Laboratory of Catalysis, School of Chemical and Environment Science, Shaanxi University of Technology, Hanzhong, Shaanxi 723001, China.
Email: wangrui830413@163.com

Zhuqing Wang, Analytical and Testing Center, Sichuan University of Science and Engineering, Zigong 643000, Sichuan Province, China.
Email: wangzq128@163.com

Makroni Lily, Key Laboratory for Macromolecular Science of Shaanxi Province, School of Chemistry and Chemical Engineering, Shaanxi Normal University, Xi'an, Shaanxi 710062, China.
Email: lilymakroni@outlook.com

Funding information
Education Department of Shaanxi Province, Grant/Award Numbers: 18JK0147, 18JS022; Natural Science Foundation of Shaanxi Province, Grant/Award Number: 2019JQ-880; Science and Technology Commission of Shanghai Municipality, Grant/Award Number: 16DZ2270100

Abstract

Quantum chemical calculations at B3LYP and CCSD(T) levels have been performed to investigate the effects of *X* (*X* = H_2O, $(H_2O)_2$, NH_3, and $H_3N\cdots H_2O$) on HNO_3 formation by the direct ($HO_2 + NO \rightarrow HNO_3$) and indirect ($N_2O_4 + H_2O \rightarrow HONO + HNO_3$) reaction of $HO_2 + NO$. The results show that, for the direct H_2O-assisted reaction, the entrance of $H_2O\cdots HO_2$ and NO is more important than the three other channels of $HO_2\cdots H_2O + NO$, $H_2O\cdots NO + HO_2$, and $NO\cdots H_2O + HO_2$. In the $H_2O\cdots HO_2 + NO$ reactions, $(H_2O)_2$, NH_3, and $H_3N\cdots H_2O$ have also been taken into account and substituted in place of H_2O; however, their contributions are negligible compared with the $H_2O\cdots HO_2 + NO$ reaction. It is noted that the atmospheric gas-phase reaction of $H_2O\cdots HO_2 + NO$ is not only competitive with the $HO_2 + NO_2 \rightarrow HNO_3$ reaction but can also compete well with the $NO_2 + HO$ reaction during the day and night at 298 K. Unlike the direct reaction assisted by *X*, the catalytic effect taken from *X* can be neglected in the indirect reaction of $N_2O_4 + H_2O \rightarrow HONO + HNO_3$. However, theoretical results of the direct and indirect reaction of $HO_2 + NO$ above may be the main reason why the yield of HNO_3 formation in $HO_2 + NO$ reaction increases experimentally in the presence of water.

KEYWORDS

atmospheric chemistry, gas-phase reaction, HO_2, NO, rate constant, reaction mechanism, troposphere

Yongqi Zhang, Aizhen Li, Mingjie Wen and Zerong Geng contributed equally to this study.

1 | INTRODUCTION

The reaction of HO_2 with NO shown in Equations (1) and (2) plays a central role in atmospheric chemistry. In the stratosphere, the reaction of Equation (1) moderates the effectiveness of the cycle involving HO_x (HO, HO_2) radicals, which is an important removal mechanism of ozone.[1–4] Meanwhile, Equation (2), the route of HNO_3 formation, although very low, has a significant impact on the atmospheric concentrations of HO_x, NO_x, HNO_3, and ozone species.[3,5–7]

$$HO_2 + NO \rightarrow NO_2 + OH \quad (1)$$

$$HO_2 + NO \rightarrow HNO_3 \quad (2)$$

Given the importance of the HO_2 + NO reaction in the atmosphere, several publications have been investigated, and as a result, the kinetics of this reaction has been studied experimentally[8–13] and theoretically[14–21] for a range of temperature. Meanwhile, as the significant enhancement[22–24] of H_2O in the HO_2 self-reaction is explained by the formation of the $H_2O\cdots HO_2$ complex, a similar mechanism may occur in other HO_2 radical reactions, particularly in Equation (2). In Equation (2), H_2O may have an obvious effect by increasing the stability of reactant complexes, reducing the activation energy of transition states,[25] and having obviously solvent effects on the chemical reaction.[26–29] Thus, Butkovskaya et al.[7] studied the effects of water monomer on the HO_2 + NO → HNO_3 reaction. In their work, the influence of water vapor on the production of HNO_3 in the gas-phase HO_2 + NO reaction was determined at 298 K using a high-pressure turbulent flow reactor coupled with a chemical ionization mass spectrometer. The yield of HNO_3 was found to increase linearly with the increase of water concentration, reaching an enhancement factor of about 8 at $[H_2O]$ 4.50×10^{17} molecules cm^{-3} (~50% relative humidity). In addition, Butkovskaya et al[7] found the rate constant of the $H_2O\cdots HO_2$ + NO → HNO_3 + H_2O reaction in the presence of water monomer to be approximately 40 times higher than the rate constant of the HO_2 + NO → HNO_3 reaction without water molecule. These investigations provide meaningful information about the mechanisms and kinetics for the HO_2 + NO → HNO_3 reaction without and with a single water molecule under atmospheric conditions. However, for this reaction with a single water molecule, the investigations discussed above only involve bimolecular reaction of $H_2O\cdots HO_2$ + NO. Until now, the three other bimolecular reactions of $HO_2\cdots H_2O$ + NO, $H_2O\cdots NO$ + HO_2, and $NO\cdots H_2O$ + HO_2 have not been involved in a water-medium HO_2 + NO → HNO_3 reaction. Indeed, in previous water-medium A + B reactions,[30–42] both the bimolecular reactions of $A\cdots H_2O$ + B and $B\cdots H_2O$ + A have not been neglected. So, it is unclear whether the water-assisted reaction mechanism of the HO_2 + NO → HNO_3 can have a positive influence on the reaction. Besides, it is also noted that water molecules play an important role in promoting the formation of HNO_3 through the indirect HO_2 + NO reaction shown in Equation (1), occurring through the hydrolysis of the NO_2 dimer. This indirect reaction of HO_2 + NO may also be one reason why the yield of HNO_3 formation in HO_2 + NO reaction increases in the presence of water.[7] In addition to water monomer, some recent works addressed the potential role of water dimer,[37,39,43] which may play a significant role in hydrogen abstraction reactions and hydrolysis reactions as the concentration[44] of $(H_2O)_2$ is up to 9×10^{14} molecules cm^{-3} at 292 K. These situations stimulated our interest in modeling the effects of H_2O and $(H_2O)_2$ on HNO_3 formation through the direct (HO_2 + NO → HNO_3) and indirect (N_2O_4 + H_2O → HONO + HNO_3) reactions of HO_2 + NO.

Recently, several groups showed that NH_3 has similar medium effects as H_2O in many atmospheric reactions.[45–49] Based on these facts, the effect of NH_3 participating in the HNO_3 formation via the direct (HO_2 + NO → HNO_3) and indirect (N_2O_4 + H_2O → HONO + HNO_3) reactions of HO_2 + NO has been investigated, and the medium of NH_3 was proven to effectively compete with an already known neutral medium (H_2O) in the lower troposphere. Indeed, it is important to mention here that, in atmospheric conditions, the average concentration of NH_3 has been investigated within the range of 0.1 to 10 ppbv.[50–52] Moreover, under certain extreme conditions, the local concentration of NH_3 is up to 2900 ppbv near open-air cattle feeding facilities.[53] From these data, it is evident that NH_3 can play an important role in various chemical reactions in the lower troposphere. Surprisingly, despite such an encouraging result, to the best of our knowledge, there has not been any further investigation to date that estimates the impact of NH_3 as a medium in the atmospheric formation of HNO_3 from the direct (HO_2 + NO → HNO_3) and indirect (N_2O_4 + H_2O → HONO + HNO_3) reactions of HO_2 + NO. Meanwhile, the bimolecular complex $H_3N\cdots H_2O$ would become the potential medium for the formation of HNO_3 via direct (HO_2 + NO → HNO_3) and indirect (N_2O_4 + H_2O → HONO + HNO_3) reactions of HO_2 + NO and shows evidence for the reactions[47,54] of CH_3O → CH_2OH and H_2CO_3 → CO_2 + H_2O reaction channels in the presence of $H_3N\cdots H_2O$, which can compete with water monomer and water dimer. So, it is very necessary to consider the effects of $H_3N\cdots H_2O$ in basic medium, which assisted the formation of HNO_3 via the direct and indirect reactions of HO_2 + NO.

In the present work, we first consider the effect of H_2O, $(H_2O)_2$, NH_3, and $H_3N\cdots H_2O$ on HNO_3 formation by the direct (HO_2 + NO → HNO_3) and indirect (N_2O_4 + H_2O → HONO + HNO_3) reactions of HO_2 + NO. Then, we completely estimate the importance of HNO_3 formation pathways from the direct and indirect reactions of HO_2 + NO in these atmospheric neutral and basic media. The present study aims to verify whether H_2O, $(H_2O)_2$, NH_3, and $H_3N\cdots H_2O$ can effectively affect the formation routes of HNO_3 and to provide insight into the detailed mechanisms and kinetics of the possible processes of HNO_3 formation in the presence of these neutral and basic species. Therefore, the present investigation has wide applications in the understanding of the formation of the HNO_3 and the gas-phase reaction of other NO_x in the atmosphere.

2 | COMPUTATIONAL METHODS

2.1 | Electronic structure calculations

The B3LYP functional[55,56] has proven to be a reliable DFT method for describing the geometries, zero-point energies (ZPEs), and frequencies for the HO_2 + NO reaction in previous studies.[7,21] As a result, the geometries of all the stationary points, including reactants, complexes, transition states (TSs), and products for the HO_2 + NO reaction without and with medium *X* (*X* = H_2O, $(H_2O)_2$, NH_3, and $H_3N\cdots H_2O$), are optimized at the B3LYP/6-311 + G(2*df*,2*p*) level, carried out using the Gaussian 09 program package.[57] Harmonic vibrational frequencies have been calculated at the same level to determine the minimum energy equilibrium structures, which possess all real frequencies, while the TS has a single imaginary frequency. Intrinsic reaction coordinate calculations[58–60] at the same level were performed to confirm that the TS connects with the desired reactants and products. To improve accuracy of the relative energies, single-point energy calculations are computed at the CCSD(T)-F12a[61,62]/VTZ-F12[63] level based on the B3LYP/6-311 + G(2*df*,2*p*) optimized geometries, performed using the ORCA software.[64] To check the reliability of the CCSD(T)-F12a/VTZ-F12 method, the T_1 diagnostic[65] of the CCSD wave function has been carried out, listed in Table S1. The T_1 diagnostic values of the closed-shell and open-shell stationary points are respectively less than 0.020 and 0.044, revealing that the CCSD wave functions in this work are reliable.

2.2 | Kinetics calculation

A general reaction scheme for medium *X*-assisted HO_2 + NO reaction can be expressed as:

$$\underset{(A)}{\text{Reactant}} + \underset{(B)}{\text{Reactant}} + \underset{(X)}{\text{catalyst}} \underset{k_{-1}}{\overset{k_1}{\rightleftharpoons}} \underset{(AX)}{\text{Bimolecular complex}} + \text{B} \underset{k_{-1}}{\overset{k_1}{\rightleftharpoons}} \underset{(AXB)}{\text{Trimolecular complex}} \overset{k_{uni}}{\rightarrow} \underset{(P+X)}{\text{Products}} \tag{3}$$

In the above scheme, it is assumed that the bimolecular complex A*X* is in equilibrium with isolated reactant A and medium *X*, and trimolecular complex AXB is in equilibrium with bimolecular complex A*X* and reactant B. Subsequently, trimolecular complex AXB undergoes unimolecular transformation to give the final product. This kinetic model is reasonably correct at the high-pressure limit, where the prereactive complex can be stabilized by collisions with other atmospherics species.[66] This method was widely used in many atmospheric reactions[31,32,66–68] assisted by media of H_2O and NH_3, and the predicted rate constants are in reasonably good agreement with the experimental values. Under pre-equilibrium approximation, the sequential bimolecular reaction rate (*v*) for the A + *X* + B reaction in the above scheme can be given as follows:

$$v = K_{eq1} \times K_{eq2} \times k_{uni} \times [A] \times [B] \times [X] = K_{eq1} \times k \times [A] \times [B] \times [X] \tag{4}$$

In this work, *k* is the product of K_{eq2} and k_{uni}. The equilibrium constants K_{eq1} and K_{eq2} are respectively given by Equations (5) and (6). The value of k_{uni} is given in Equation (7) and can be calculated by using the conventional variational TS theory (CVT)[69,70] as implemented in Polyrate 8.2 programs[71]:

$$K_{eq1}(T) = \sigma \frac{Q_{AX}}{Q_A Q_X} \exp\left(\frac{E_A + E_X - E_{AX}}{RT}\right) \tag{5}$$

$$K_{eq2}(T) = \sigma \frac{Q_{AXB}}{Q_{AX} Q_B} \exp\left(\frac{E_{AX} + E_B - E_{AXB}}{RT}\right) \tag{6}$$

$$k_b = \sigma \kappa_{SCT} \frac{k_B T Q_{TS}^{\neq}(T,s)}{h \, Q_{AXB}(T)} \exp\left(-\frac{V_{MEP}(s)}{k_B T}\right) \tag{7}$$

where in Equations (5) and (6), Q_{AXB}, Q_{AX}, Q_A, and Q_X denote the partition functions of the trimolecular complex AXB, the two-body complex A*X*, reactants A and medium *X*, respectively; E_{AXB}, E_{AX}, E_A, and E_X stand for the energies of the species of AXB, A*X*, A and *X*, respectively; and σis the degeneracy of the reaction channel. In Equation (7), it is noted that κ_{SCT} is the small curvature tunneling (SCT) correction[72] as implemented in Polyrate 8.2 programs; *h* is the Planck's constant, k_B is the Boltzmann constant; $V_{MEP}(s)$ is the classical barrier height for the variational TS; and $Q_{TS}^{\neq}$ and Q_{AXB} are the total partition functions for the TS and the trimolecular complex AXB, respectively.

3 | RESULTS AND DISCUSSION

In this work, we have tried to determine the atmospheric fate of HNO_3 by investigating the direct (HO_2 + NO → HNO_3) and indirect (N_2O_4 + H_2O → HONO + HNO_3) reactions of HO_2 + NO without and with medium *X* through electronic structure and rate coefficient calculations. The TS in the HO_2 + NO reaction was denoted by "TS" followed by a number, whereas the pre-reactive complex in each reaction channel was respectively labeled by "IM" followed by a number. Species in direct and indirect reactions of HO_2 + NO have been denoted respectively by "a" and "b" suffixes. Besides, species in the presence of H_2O, $(H_2O)_2$, NH_3, and $H_3N\cdots H_2O$ were respectively denoted by a "WM," "WD," "AM," and "AW" as a suffix.

3.1 | Uncatalyzed HO_2 + NO → HNO_3 reaction

The HO_2 + NO → HNO_3 reaction was theoretically reported in the previous studies.[7,21] In this study, we have reinvestigated this reaction at the CCSD(T)-F12a/VTZ-F12//B3LYP/6-311+ G(2*df*,2*p*) level in order to confirm the effect of medium *X* (*X* = H_2O, $(H_2O)_2$, NH_3, and $H_3N\cdots H_2O$). As seen, the HO_2 + NO → HNO_3 reaction is initiated by HO_2 binding with NO to form a complex of *trans*-HO_2-NO (Figure 1, labeled as IM1a) with a binding energy of 22.9 kcal mol^{-1} (Table S1), which subsequently forms HNO_3 through a TS, TS1a, with a barrier height of 23.8 kcal mol^{-1}. The stabilization energy of HNO_3 for isolated reactants was found to be 54.9 kcal mol^{-1}. Compared to the previous theoretical reports, the present geometrical structures match well with the results of earlier investigations[7,21]; however, the energy values are different from previously reported results.[7,21] The reason might be due to the inclusion of single-point energy calculations in present studies, as well as a different quantum chemical method being used for energetic calculations. As quantitative barrier heights for complex atmospheric reactions can be obtained using W3X-L,[73–76] the single-point energy calculations have also been performed at the W2X and W3X-L levels of theory to estimate the error bars of CCSD(T)-F12a/VTZ-F12 for the HO_2 + NO → HNO_3 reaction. It is shown in Table S2 that the unsigned error of CCSD(T)-F12a/VTZ-F12 is less than 0.8 kcal mol^{-1} when compared with W3X-L results. Therefore, the affordable CCSD(T)-F12a/VTZ-F12 method is chosen to calculate single-point energy for the HO_2 + NO → HNO_3 reaction without and with medium *X*.

3.2 | H_2O-mediated HO_2 + NO → HNO_3 reaction

When the H_2O monomer is introduced in the HO_2 + NO → HNO_3 reaction, four bimolecular reactions shown in Equations (8) to (11) have been taken into account. The optimized geometric structures of the HO_2 + NO → HNO_3 reaction with H_2O are shown in Figure S2, and its corresponding schematic energy diagram have been displayed in Figures 2 and S1. As seen in Figures 2 and S1, the complexes of $H_2O\cdots HO_2$ and $HO_2\cdots H_2O$ are more stable than $H_2O\cdots$NO and NO$\cdots H_2O$, which indicate that NO exhibits hydrophobicity toward water. Compared with the HO_2 + NO → HNO_3 reaction without medium, the energy barrier of TS_WM2a (Figure S1) and TS_WM4a (Figure S1) for the isolated reactants respectively increases by 2.9 and 3.6 kcal mol^{-1}. Thus, here, the bimolecular reactions of $H_2O\cdots HO_2$ + NO (Channel R_WM1*a*), and $H_2O\cdots$NO + HO_2 (Channel R_WM3*a*) shown in Figure 2 are only considered in the HO_2 + NO + H_2O reaction.

$$H_2O\cdots HO_2 + NO \rightarrow HONO_2 + H_2O \text{ (Channel R\_WM1}a\text{)} \quad (8)$$

$$HO_2\cdots H_2O + NO \rightarrow HONO_2 + H_2O \text{ (Channel R\_WM2}a\text{)} \quad (9)$$

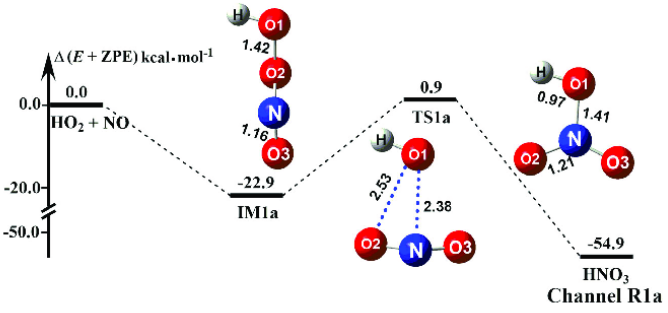

FIGURE 1 Schematic energy diagram for the HO_2 + NO → HNO_3 reaction at the CCSD(T)-F12a/ VTZ-F12//B3LYP/6-311+G(2*df*,2*p*) level

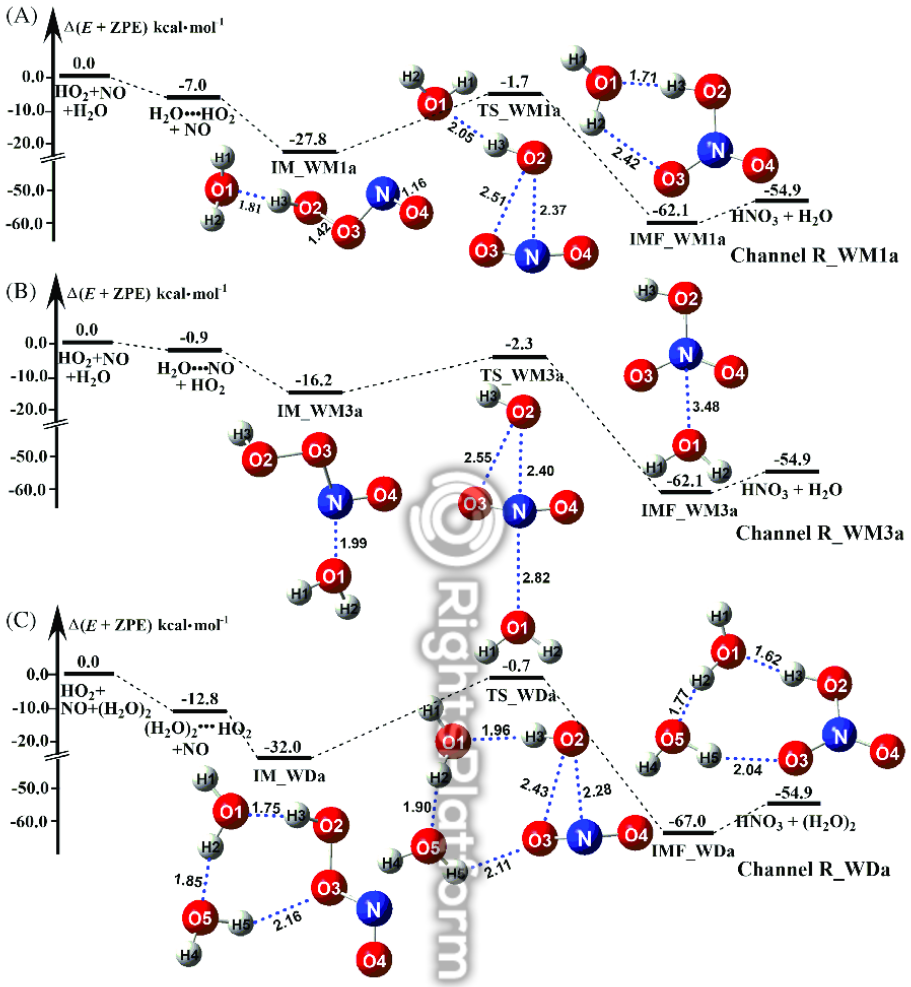

FIGURE 2 Schematic energy diagrams for water-catalyzed HO_2 + NO → HNO_3 reactions occurring through: A, $H_2O\cdots HO_2$ + NO; B, $H_2O\cdots$NO + HO_2; and C, $(H_2O)_2\cdots HO_2$ + NO channels at the CCSD(T)-F12a/VTZ-F12//B3LYP/6-311+G(2*df*,2*p*) level

$$H_2O\cdots NO + HO_2 \rightarrow HONO_2 + H_2O \text{ (Channel R\_WM3}a\text{)} \quad (10)$$

$$NO\cdots H_2O + HO_2 \rightarrow HONO_2 + H_2O \text{ (Channel R\_WM4}a\text{)} \quad (11)$$

The reaction of Channel R_WM1*a* reported here is in good agreement with the previous work[7] geometrically and energetically. As shown in Figure 2A, Channel R_WM1*a* starts with the formation of the prereactive complex IM_WM1a with the binding energy of 27.8 kcal mol^{-1} relative to the H_2O + HO_2 + NO reactants, which is stable by 4.9 kcal mol^{-1} than that of IM1a relative to the HO_2 + NO reactants. This indicates that H_2O enhances the stability of the reactant complex greatly. As shown in Figure 2, complex IM_WM1a shows a chain configuration, where only one hydrogen-bonded (O1···H3, 1.81 Å) interaction was involved between the H_2O and IM1a complex. Then, following complex IM_WM1a, Channel R_WM1*a* proceeded through TS TS_WM1a to produce the six-membered ring complex of $H_2O\cdots HNO_3$ (IMF_WM1a) after climbing the barrier height of 26.1 kcal mol^{-1}. Compared with the TS TS1a without a mediator, the additional water molecule in TS TS_WM1a is hydr4ogen bonded to the H atom of one HO_2 group in *trans*-HO_2-NO complex. From an energetic point of view, Channel R_WM1*a* can occur easily with an

activation energy of −1.7 kcal mol^{-1}, which is lower by 2.6 kcal mol^{-1} than the naked reaction of HO_2 + NO → HNO_3. This result indicates that a single water molecule in Channel R_WM1*a* can exert a positive mediation role in reducing the energy barrier of the HO_2 + NO → HNO_3 reaction.

Regarding Channel R_WM3*a*, the chain complex IM_WM3a was formed in the first step. From a geometrical point of view, compared with IM1a complex, a van der Waals interaction (O1···N, 1.99 Å) is involved in complex IM_WM3a with a binding energy of 16.2 kcal mol^{-1}. Starting from complex IM_WM3a, Channel R_WM3*a* proceeds through TS TS_WM3a to form a complex of IMF_WM3a. As depicted in Figure 2B, TS_WM3a has a calculated energy barrier height of −2.3 kcal mol^{-1} relative to isolated reactants. Compared with the TS1a without a mediator, the additional water molecule in TS_WM1a is conducive to the occurrence of isomerization of trans-HOONO to HNO_3 with an energy lower by 3.2 kcal mol^{-1}. Moreover, for isolated reactants, the energy barrier of Channel R_WM3*a* is lower by 0.6 kcal mol^{-1} than that of Channel R_WM1*a*. This indicates that the occurrence of Channel R_WM3*a* is easier than Channel R_WM1*a* energetically. To check whether Channel R_WM1*a* is more favorable than Channel R_WM3*a* or not, it is necessary to calculate the rate ratio between Channel R_WM1*a* and Channel R_WM3*a*. For the HO_2 + NO + H_2O reaction, the rate via the H_2O···HO_2 + NO (Channel R_WM1*a*) and H_2O···NO + HO_2 (Channel R_WM3*a*) reactions are respectively expressed in Equations (12) and (13).

$$v_{R\_WM1a} = \frac{d[HONO_2]}{dt} = K_{eq1a} \times k_{R\_WM1a} \times [HO_2] \times [NO] \times [H_2O] \quad (12)$$

$$v_{R\_WM3a} = \frac{d[HONO_2]}{dt} = K_{eq1b} \times k_{R\_WM3a} \times [HO_2] \times [NO] \times [H_2O] \quad (13)$$

where K_{eq1a} and K_{eq1b} are respectively the equilibrium constants for the formation of H_2O···HO_2 and H_2O···NO, and k_{R_WM1a} and k_{R_WM3a} are respectively the bimolecular rate constants of Channel R_WM1*a* and Channel R_WM3*a*. The calculated rate ratio v_{R_WM1a}/v_{R_WM3a} of the HO_2 + NO + H_2O reaction shows that the entrance of H_2O···HO_2 and NO is more important than that of H_2O···NO and HO_2 because the rate ratio v_{R_WM1a}/v_{R_WM3a} is 1.81 × 10^2 at 298 K (Table 1). As a result, $(H_2O)_2$, NH_3, and H_3N···H_2O-mediated HO_2 + NO → HNO_3 reaction has only been taken into account with the substitution of H_2O in Channel R_WM1*a* respectively by $(H_2O)_2$, NH_3, and H_3N···H_2O.

3.3 | $(H_2O)_2$ mediated the HO_2 + NO → HNO_3 reaction

Figure 2C shows the schematic energy diagram for $(H_2O)_2$-mediated HO_2 + NO → HNO_3 reaction, where the corresponding channel is labeled as Channel R_WD*a*, and its rate constant is listed in Table S5. $(H_2O)_2$-mediated Channel R_WD*a*, similar to the H_2O-mediated Channel R_WM1*a*, proceeds via the initial formation of IM_WDa complex through the reaction between $(H_2O)_2$···HO_2 and NO (Figure 2C). The stabilization energy of IM_WDa was found to be 32.0 kcal mol^{-1} for the isolated reactants, where $(H_2O)_2$ enhances the stability of the reactant complex IM1a by 9.1 kcal mol^{-1}. Then, the IM_WDa has been converted to give complex IMF_WDa with the stability of 67.0 kcal mol^{-1} via an eight-membered

TABLE 1 The equilibrium constants (molecules^{-1} cm^{-3}), rate constants (cm^3 molecules^{-1} s^{-1}), and the rate ratio for H_2O, $(H_2O)_2$, NH_3, and H_2O···NH_3-catalyzed direct (HO_2 + NO → HNO_3) and indirect (N_2O_4 + H_2O → HONO + HNO_3) reactions of HO_2 + NO at 298 K

K_{eq1a}	k_{R_WM1a}	K_{eq1b}	k_{R_WM3a}	K_{eq1c}	k_{R_WDa}
3.08E-20	1.74E-13	1.35E-22	2.10E-13	1.85E-17	8.24E-21
K_{eq1d}	k_{R_AMa}	K_{eq1e}	k_{R_AW1a}	K_{eq1f}	k_{R_AW2a}
3.56E-18	6.07E-16	9.09E-21	1.75E-16	6.54E-19	2.21E-19
v_{R_WM1a}/v_{R_WM3a}	v_{R_WM1a}/v_{R_WDa} (20% RH)	v_{R_WM1a}/v_{R_WDa} (100% RH)	v_{R_AW1a}/v_{R_AW2a}	v_{R_AMa}/v_{R_AW1a}	v_{R_WM1a}/v_{R_AMa} (10ppbv-20%RH)
1.81E+02	9.74E+07	1.93E+07	1.10E+01	2.01E+06	1.49E+06
v_{R_WM1a}/v_{R_AMa} (2900ppbv-20%RH)	v_{R_WM1a}/v_{R_AMa} (10ppbv-100%RH)	v_{R_WM1a}/v_{R_AMa} (2900ppbv-100%RH)	k_{R1b}	k_{R_WMb}	k_{R_WDb}
5.24E+03	7.64E+06	2.69E+04	1.02E-18	6.82E-19	5.69E-15
k_{R_AMb}	k_{R_AWb}	v_{R_WMb}/v_{R1b}	v_{R_WDb}/v_{R1b}	v_{R_AMb}/v_{R1b}	v_{R_AWb}/v_{R1b}
2.78E-17	9.65E-19	1.15E-05	1.98E-04	6.40E-06	3.65E-10

Note: K_{eq1a}, K_{eq1b}, K_{eq1c}, K_{eq1d}, K_{eq1e}, and K_{eq1f} are respectively the equilibrium constant for the formation of H_2O···HO_2, H_2O···NO, HO_2···$(H_2O)_2$, H_3N···HO_2, H_3N···H_2O···HO_2-1, and H_3N···H_2O···HO_2-2; k_{R_WM1a}, k_{R_WM3a}, k_{R_WDa}, k_{R_AMa}, k_{R_AW1a}, k_{R_AW2a}, k_{R1b}, k_{R_WMb}, k_{R_WDb}, k_{R_AMb}, and k_{R_AWb} are respectively the bimolecular rate constant of Channel R_WM1*a*, Channel R_WM3*a*, Channel R_WD*a*, Channel R_AM*a*, Channel R_AW1*a*, Channel R_AW2*a*, Channel R1*b*, Channel R_WM*b*, Channel R_WD*b*, Channel R_AM*b*, and Channel R_AW*b*.

cyclic TS_WDa (−0.7 kcal mol^{-1}). From an energetic point of view, the energy barrier for this reaction is 1.0 kcal mol^{-1} lower than H_2O-mediated (Channel R_WM1*a*) channel. The rate constant (k_{R_WDa}) for this channel was calculated to be 8.24×10^{-21} cm^3·molecule^{-1} s^{-1} at 298 K, which is ~10^7 times lower than the H_2O-mediated channel (Table 1). To check the competition of Channel R_WD*a* with Channel R_WM1*a*, it is necessary to calculate the rate ratio between Channel R_WM1*a* and Channel R_WD*a* as shown in Equation (14).

$$\frac{v_{R\_WM1a}}{v_{R\_WDa}} = \frac{K_{eq1a} \times k_{R\_WM1a} \times [HO_2] \times [NO] \times [H_2O]}{K_{eq1c} \times k_{R\_WDa} \times [HO_2] \times [NO] \times [(H_2O)_2]} = \frac{K_{eq1a} \times k_{R\_WM1a} \times [H_2O]}{K_{eq1c} \times k_{R\_WDa} \times [(H_2O)_2]} \quad (14)$$

The calculated rate ratio v_{R_WM1a}/v_{R_WDa} shows that the $H_2O\cdots HO_2$ + NO is more important than that of the $(H_2O)_2\cdots HO_2$ + NO reaction because the rate ratio v_{R_WM1a}/v_{R_WDa} is 1.93×10^7 at 298 K (Table 1). This finding is not surprising—after all, the concentration of $(H_2O)_2$ is much lower compared to that of H_2O, and the value of k_{R_WDa} is also much smaller than that of k_{R_WM1a}.

3.4 | NH_3 and $H_3N\cdots H_2O$-mediated HO_2 + NO → HNO_3 reaction

The schematic energy diagrams for NH_3 (Channel R_AM*a*) and $H_3N\cdots H_2O$ (Channel R_AW1*a* and Channel R_AW2*a*)-mediated HO_2 + NO → HNO_3 reaction have been displayed in Figure 3, and their calculated rate constants are listed in Table S5. As shown in Figure 3A, from a

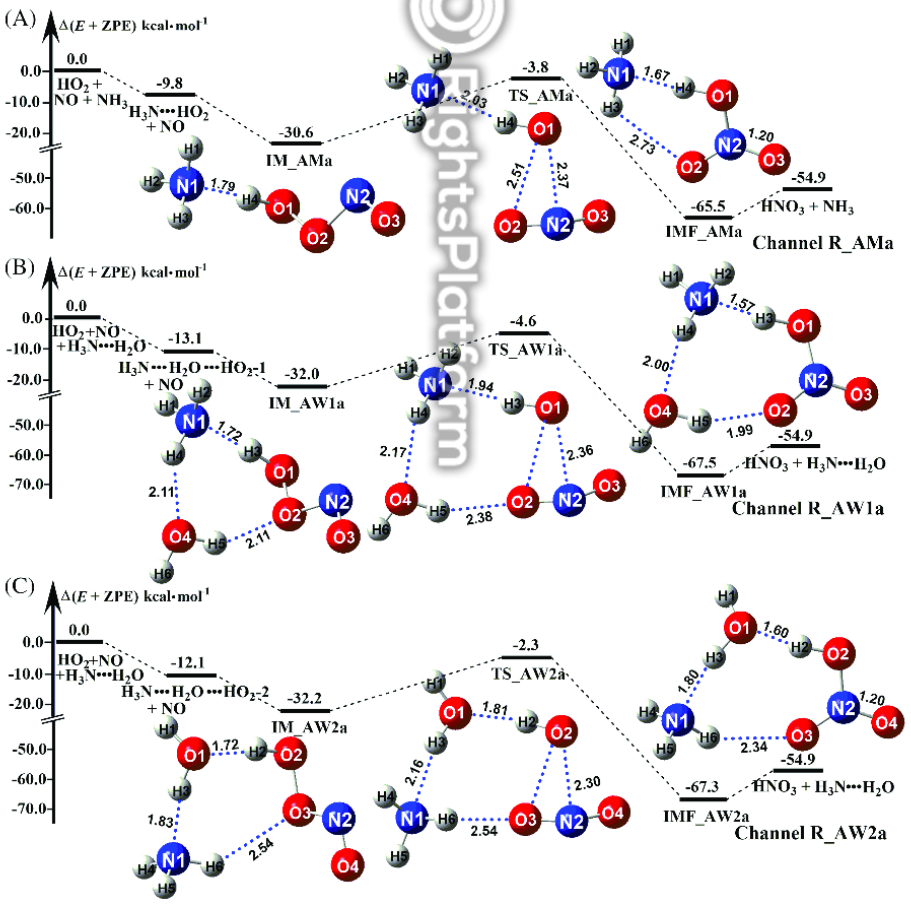

FIGURE 3 Schematic energy diagrams for ammonia-catalyzed HO_2 + NO → HNO_3 reaction occurring through: A, $H_3N\cdots HO_2$ + NO; B, $H_3N\cdots H_2O\cdots HO_2$-1 + NO; and C, $H_3N\cdots H_2O\cdots HO_2$-2 + NO channels at the CCSD(T)-F12a/VTZ-F12//B3LYP/6-311 + G(2*df*,2*p*) level

geometrical point of view, the structures of the prereactive complex, TS, and postreactive complex in NH_3-catalyzed $HO_2 + NO \rightarrow HNO_3$ reaction are similar to those determined for water-mediated Channel R_WM1*a*, as shown in Figure 2A with NH_3 replacing H_2O. From an energetic point of view, NH_3 has a more obvious medium effect than H_2O, for example, compared with H_2O-mediated reaction, the stability of complex IM_AMa increases by 2.8 kcal mol^{-1}; meanwhile, the activation energy of TS TS_AMa decreases by 2.1 kcal mol^{-1}.

Figure 3B,C show the potential energy profile and the corresponding equilibrium geometries for the reaction of HO_2 + NO in the presence of $H_3N\cdots H_2O$. Two prereactive complexes, IM_AW1a (Channel R_AW1*a*) and IM_AW2a (Channel R_AW2*a*), are very similar in structure to complex IM_WDa, with NH_3 used in place of one of the two water molecules in complex IM_WDa. The binding energies of IM_AW1a and IM_AW2a, from the separate molecules, are 32.0 and 32.2 kcal mol^{-1}, respectively. $H_3N\cdots H_2O$ in complex IM_AW1a and IM_AW2a enhances the stability of the reactant complex IM1a by 9.1 to 9.3 kcal mol^{-1}, which are close to the stability of $(H_2O)_2$ in complex IM_WDa. The formation of postreactive complex IMF_AW1a from complex IM_AW1a of Channel R_AW1*a* through a TS TS_AW1a with an energy barrier of −4.6 kcal mol^{-1} is decreased by 3.9 kcal mol^{-1} compared with the TS TS_WDa obtained for $(H_2O)_2$ that participates in the reaction. Regarding Channel R_AW2*a*, starting with the reactant complex IM_AW2a, the reaction occurs through the TS TS_AW2a to form the product complex IMF_AW2a. The energy barrier of TS_AW2a with respect to isolated reactants is −2.3 kcal mol^{-1}, which is higher by 2.3 kcal mol^{-1} than that of TS_AW1a. Furthermore, the product complex IMF_AW1a is less stable than IMF_AW2a by 0.2 kcal mol^{-1}.

The competition between Channel R_AW1*a* and Channel R_AW2*a* has been proven by the rate ratio between Channel R_AW1*a* and Channel R_AW2*a*, as shown in Equation (15), where the rate ratio v_{R_AW1a}/v_{R_AW2a} is 11.00 at 298 K (Table 1). This reveals that, $H_3N\cdots H_2O$ participates in the HO_2 + NO → HNO_3 reaction, and so, Channel R_AW1*a* is more favorable than Channel R_AW2*a*. Meanwhile, the calculated rate ratio v_{R_AMa}/v_{R_AWla}, as shown in Equation (16), suggests that the $H_3N\cdots HO_2$ + NO is more important than that of $H_3N\cdots H_2O\cdots HO_2$ and NO because the rate ratio v_{R_AMa}/v_{R_AW1a} is 2.01×10^6 at 298 K (Table 1). This finding is similar to the water medium reaction, where H_2O is preferred than $(H_2O)_2$. Furthermore, it is interesting to compare the mediated effect between H_2O and NH_3. The calculated result shows that the contribution of the $H_3N\cdots HO_2$ + NO route can be neglected as the rate ratio v_{R_WM1a}/v_{R_AMa} shown in Equation (17) is still up to 2.69×10^4 at 298 K (Table 1) even when the concentration of NH_3 is up to 2900 ppbv.

$$\frac{v_{R\_AW1a}}{v_{R\_AW2a}} = \frac{K_{eq1e} \times k_{R\_AW1a} \times [HO_2] \times [NO] \times [H_3N\cdots H_2O]}{K_{eq1f} \times k_{R\_AW2a} \times [HO_2] \times [NO] \times [H_3N\cdots H_2O]} = \frac{K_{eq1e} \times k_{R\_AW1a}}{K_{eq1f} \times k_{R\_AW2a}} \tag{15}$$

$$\frac{v_{R\_AMa}}{v_{R\_AW1a}} = \frac{K_{eq1d} \times k_{R\_AMa} \times [HO_2] \times [NO] \times [H_3N]}{K_{eq1f} \times k_{R\_AW1a} \times [HO_2] \times [NO] \times [H_3N\cdots H_2O]} = \frac{K_{eq1d} \times k_{R\_AMa} \times [H_3N]}{K_{eq1f} \times k_{R\_AW1a} \times [H_3N\cdots H_2O]} \tag{16}$$

$$\frac{v_{R\_WM1a}}{v_{R\_AMa}} = \frac{K_{eq1a} \times k_{R\_WM1a} \times [HO_2] \times [NO] \times [H_2O]}{K_{eq1d} \times k_{R\_AMa} \times [HO_2] \times [NO] \times [H_3N]} = \frac{K_{eq1a} \times k_{R\_WM1a} \times [H_2O]}{K_{eq1d} \times k_{R\_AMa} \times [H_3N]} \tag{17}$$

3.5 | H_2O, $(H_2O)_2$, NH_3, and $H_3N\cdots H_2O$-mediated $N_2O_4 + H_2O \rightarrow HONO + HNO_3$ reaction

The $N_2O_4 + H_2O \rightarrow HONO + HNO_3$ reaction has been regarded as an indirect source of HNO_3 formation by the reaction of HO_2 + NO. The hydrolysis reaction of N_2O_4 without and with H_2O, $(H_2O)_2$, NH_3, and $H_2O\cdots NH_3$ has been investigated before.[77] Here, calculations for the favorable routes of this reaction in the presence of H_2O, $(H_2O)_2$, NH_3, and $H_2O\cdots NH_3$ were also performed to compare with the corresponding reaction of HO_2 + NO → HNO_3 in the presence of H_2O, $(H_2O)_2$, NH_3, and $H_2O\cdots NH_3$. Thus, Figure 4 shows the PESs for the *t*-$N_2O_4 + H_2O$ reaction in the presence of H_2O, $(H_2O)_2$, NH_3, and $H_2O\cdots NH_3$, and Table 1 lists their rate constants at 298 K.

As seen in Figure 4, H_2O, $(H_2O)_2$, NH_3, and $H_2O\cdots NH_3$ enhance the stability of the reactant complex IM1b by 3.5 to 8.1 kcal mol^{-1}; meanwhile, they reduce the energy barrier of the TS by 1.7 to 12.6 kcal mol^{-1}. The rate ratio between the $N_2O_4 + H_2O \rightarrow HONO + HNO_3$ reaction in the presence of *X* (*X* = H_2O, $(H_2O)_2$, NH_3, and $H_3N\cdots H_2O$) and the corresponding reaction without *X* are shown in Equations (18) to (21). The calculated rate ratio shows that the $N_2O_4 + H_2O \rightarrow HONO + HNO_3$ reaction without *X* is much larger than the corresponding reaction with *X* because the rate ratio of v_{R_WMb}/v_{R1b}, v_{R_WDb}/v_{R1b}, v_{R_AMb}/v_{R1b}, and v_{R_AWb}/v_{R1b} is 1.15×10^{-5}, 1.98×10^{-4}, 6.40×10^{-6}, and 3.65×10^{-10} at 298 K, respectively (Table 1). This indicates that the catalytic effect of the $N_2O_4 + H_2O \rightarrow HONO + HNO_3$ reaction without *X* is more obvious than the corresponding reaction with *X* (*X* = H_2O, $(H_2O)_2$, NH_3, and $H_3N\cdots H_2O$), and the catalytic effect observed from *X* is neglected. However, the yield of HNO_3 formation occurring through the hydrolysis of NO_2 dimer in HO_2 + NO reaction increases in the presence of water.

$$\frac{v_{R\_WMb}}{v_{R1b}} = \frac{K_{eq1i} \times k_{R\_WMb} \times [N_2O_4] \times [H_2O] \times [H_2O]}{k_{R1b} \times [N_2O_4] \times [H_2O]} = \frac{K_{eq1i} \times k_{R\_WMb} \times [H_2O]}{k_{R1b}} \tag{18}$$

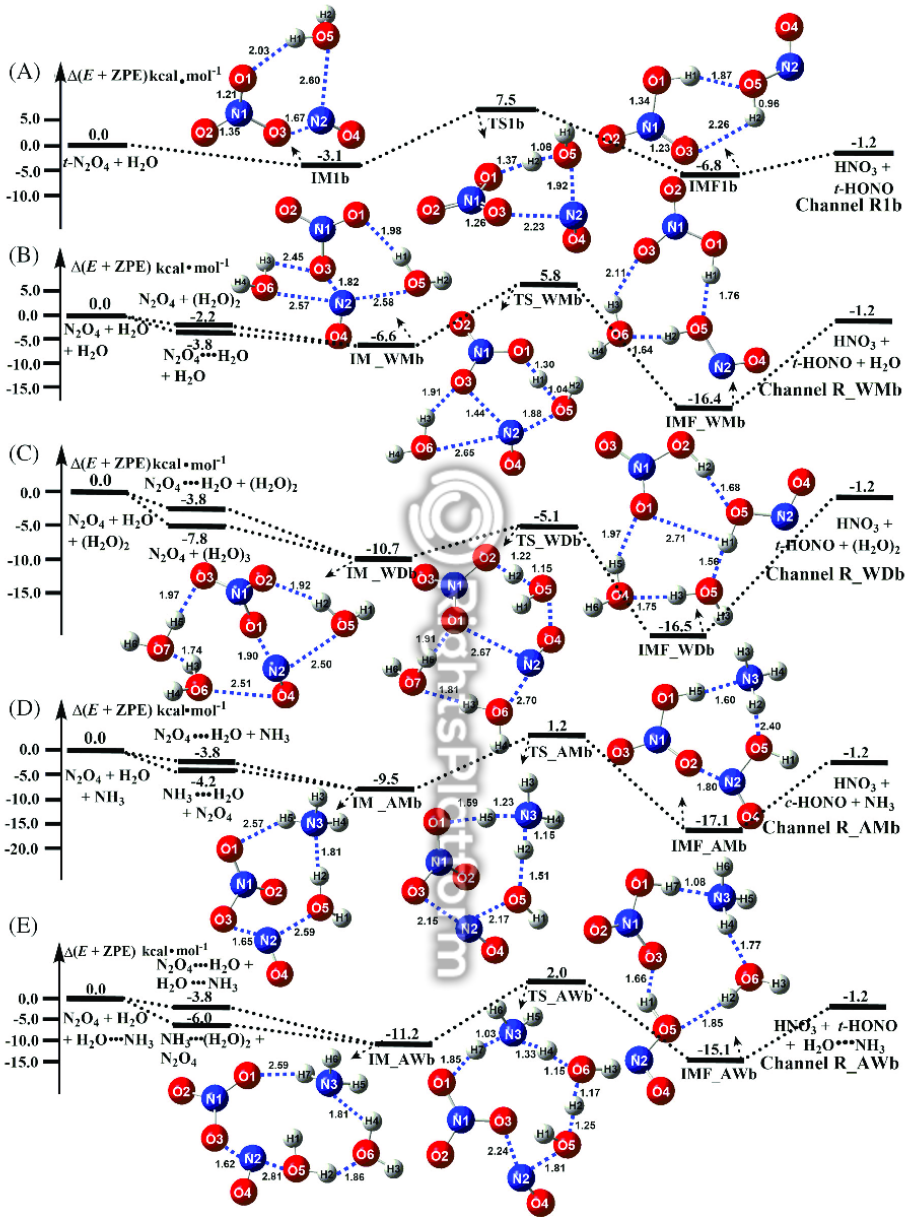

FIGURE 4 Schematic energy diagram for the $N_2O_4 + H_2O \rightarrow HNO_3 + HONO$ reaction without and with H_2O, $(H_2O)_2$, NH_3, and $H_2O\cdots NH_3$ at the CCSD(T)-F12a/VTZ-F12//B3LYP/6-311+G(2*df*,2*p*) level

$$\frac{v_{R\_WDb}}{v_{R1b}} = \frac{K_{eq1j} \times k_{R\_WDb} \times [N_2O_4] \times [H_2O] \times [(H_2O)_2]}{k_{R1b} \times [N_2O_4] \times [H_2O]} = \frac{K_{eq1j} \times k_{R\_WDb} \times [(H_2O)_2]}{k_{R1b}} \quad (19)$$

$$\frac{v_{R\_AMb}}{v_{R1b}} = \frac{K_{eq1k} \times k_{R\_AMb} \times [N_2O_4] \times [H_2O] \times [NH_3]}{k_{R1b} \times [N_2O_4] \times [H_2O]} = \frac{K_{eq1k} \times k_{R\_AMb} \times [NH_3]}{k_{R1b}} \quad (20)$$

$$\frac{v_{R\_AWb}}{v_{R1b}} = \frac{K_{eq1l} \times k_{R\_AWb} \times [N_2O_4] \times [H_2O] \times [NH_3 \cdots H_2O]}{k_{R1b} \times [N_2O_4] \times [H_2O]} = \frac{K_{eq1l} \times k_{R\_AWb} \times [NH_3 \cdots H_2O]}{k_{R1b}} \quad (21)$$

3.6 | Atmospheric implications

For the HO_2 + NO → HNO_3 reaction without *X*, its computed rate constant (k_{R1a}), as shown in Table 2, was 1.46×10^{-14} cm^3·$molecule^{-1}$ s^{-1}, which was in good agreement with experimental reports.[5,79,80] As discussed above, the $H_2O \cdots HO_2$ + NO → HNO_3 + H_2O reaction (Channel R_WM1*a*) and the N_2O_4 + H_2O → HONO + HNO_3 reaction (Channel R1*b*) are respectively the most favorable processes in the direct (HO_2 + NO → HNO_3) and indirect (N_2O_4 + H_2O → HONO + HNO_3) reactions of HO_2 + NO without and with *X* (*X* = H_2O, $(H_2O)_2$, NH_3, and $H_3N \cdots H_2O$). As for the rate ratio between Channel R_WM1*a* and Channel R1*b* seen in Table 2, v_{R_WM1a}/v_{R1b}, as shown in Equation (22), is 1.15×10^7 at 298 K. This indicates that the main sources of HNO_3 formation from HO_2 + NO reaction are obtained from the direct reaction of the $H_2O \cdots HO_2$ + NO → HNO_3 + H_2O reaction.

$$\frac{v_{R\_WM1a}}{v_{R1b}} = \frac{K_{eq1a} \times k_{R\_WM1a} \times [HO_2] \times [NO] \times [H_2O]}{k_{R1b} \times [N_2O_4] \times [H_2O]} = \frac{K_{eq1a} \times k_{R\_WM1a} \times [HO_2] \times [NO]}{k_{R1b} \times [N_2O_4]} \quad (22)$$

In gas-phase atmospheric reactions, the relevance of the $H_2O \cdots HO_2$ + NO → HNO_3 + H_2O reaction (Channel R_WM1*a*) depends heavily on its ability to compete with the HO_2 + NO → HNO_3 reaction without medium (Channel R1*a*) and NO_2 + HO → HNO_3 (Channel R2). Therefore, it is of great importance to discuss the rate ratio of v_{R_WM1a}/v_{R1a} and v_{R_WM1a}/v_{R2}. To meet this goal, rate ratios as shown in Equations (23) and (24) are listed in Table 2 at 298 K.

$$\frac{v_{R\_WM1a}}{v_{R1a}} = \frac{K_{eq1a} \times k_{R\_WM1a} \times [HO_2] \times [NO] \times [H_2O]}{k_{R1a} \times [HO_2] \times [NO]} = \frac{K_{eq1a} \times k_{R\_WM1a} \times [H_2O]}{k_{R1a}} \quad (23)$$

$$\frac{v_{R\_WM1a}}{v_{R2}} = \frac{K_{eq1a} \times k_{R\_WM1a} \times [HO_2] \times [NO] \times [H_2O]}{k_{R2} \times [NO_2] \times [HO]} \quad (24)$$

In Equations (23) and (24), k_{R1a}, k_{R_WM1a}, and k_{R2} are respectively the rate constant of Channel R1*a*, Channel R_WM1*a*, and Channel R2.[78] The rate ratio of v_{R_WM1a}/v_{R1a}, and v_{R_WM1a}/v_{R2} depends on the H_2O,[35] HO_2,[32] NO,[1] NO_2,[35] and HO[49] concentrations in the atmosphere. At 298 K, taking into account typical tropospheric concentrations of 7.7×10^{17} molecules cm^{-3} of H_2O, 3.0×10^8 molecules cm^{-3} of HO_2, 9.3×10^{15} molecules cm^{-3} of NO, 1.0×10^9 molecules cm^{-3} of NO_2, and 1.0×10^6 molecules cm^{-3} of HO, Channel R_WM1*a* can compete with Channel R1*a* (or Channel R2). As seen in Table 2, it is estimated that the $H_2O \cdots HO_2$ + NO reaction can compete well with the HO_2 + NO and NO_2 + HO reaction at 298 K because the rate ratios v_{R_WM1a}/v_{R1a} and v_{R_WM1a}/v_{R2} are respectively about 1.28 and 389.00. Besides, when the HO concentration is decreased to 10^4 molecules cm^{-3} during the night,[81] $H_2O \cdots HO_2$ + NO reaction can compete well with the NO_2 + HO reaction[82,83] at 298 K because the rate ratio v_{R_WM1a}/v_{R2} is about 3.88×10^4, as shown in Table 2. Thus, the $H_2O \cdots HO_2$ + NO reaction can contribute to the formation of HNO_3 during the day and the night at 298 K.

TABLE 2 The rate ratio of $H_2O \cdots HO_2$ + NO reaction with the reactions of HO_2 + NO → HNO_3 (Channel R1*a*) and NO_2 + HO → HNO_3 (Channel R2) at 298 K

							$v_{R\_WM1a(100\%RH)}/v_{R2}$	
T(K)	k_{R1a}	k_{R2}	k_{R_WM1a}	v_{R1a}/v_{R1b}	$v_{R\_WM1a(100\%RH)}/v_{R1a}$	$v_{R\_WM1a(100\%RH)}/v_{R1b}$	Day	Night
298	1.46E-14[a]	4.00E-11[b]	1.74E-13	5.75E+11	1.28	1.15E+07	3.89E+02	3.88E+04

[a]The rate constant of Channel R1*a* is taken from Table S3.
[b]The rate constant of Channel R2 is taken from Williams et al.[78]